**Technical Paper**

ISSN 1997-1400 Int. J. Pavement Res. Technol. 8(3):199-205


# Effect of Interaction Parameters on the Hardness and Elastic Modulus of Crumb Rubber Modified Asphalt

Mohyeldin Ragab[1], Magdy Abdelrahman[1+], and Amir Ghavibazoo[1]

**Abstract:** Instrumented indentation presents an approach to measure the mechanical properties such as hardness and elastic modulus of materials on micro and nano scale. This gives an idea about the behavior of materials during their application when they are laid as layers of thickness of the nano or micro scale level. Two advantages can be achieved from the utilization of instrumented micro-indentation on crumb rubber modified asphalt; the first would be to measure the properties of asphalt layers of thicknesses on the micro scale to simulate the behavior of thin asphalt layer on aggregate. The second advantage would be to investigate the effect of interaction (blend processing) synthesis parameters (mixing speed, temperature and time) on the final product hardness and elastic modulus. Through the current work, it was found that the interaction parameters play a major role on the determination of the hardness and elastic modulus of crumb rubber modified asphalt (CRMA). The utilization of moderate (30 Hz) to high (50 Hz) interaction speeds at low interaction temperature (160℃) resulted in minimal enhancements in both the hardness and elastic modulus. On the other hand, the utilization of moderate (190℃) interaction temperature with high interaction speed (50 Hz) resulted in major property enhancements for both the hardness and elastic modulus. At 220℃ interaction temperature, deterioration in both the hardness and elastic modulus was observed after 4 hrs of interaction time regardless of the interaction speed utilized.

**DOI**: 10.6135/ijprt.org.tw/2015.8(3).199
***Key words**: Crumb rubber modified asphalt, Interaction parameters, Microindentation.*

## Introduction

Instrumented nanoindentation and microindentation are the only methods available for direct measurements of modulus and hardness of asphalt binder film. In the work by Tarefder et al., the use of nanoindenter for testing asphalt binder, mastic, and aggregate was carried out to measure modulus and hardness of the materials [1]. In another work by Yousefi, the author used nanoindentation to examine aging factors of asphalt binder as well as the different effects of various asphalt additives and their effectiveness [2]. Tarefder et. al. used nanoindentation to compare the hardness and modulus of the mastics with varying mica content [3]. Marchildon and Hesp introduced the possibility of development of microindentation tests for the specification grading of asphalt cements [4]. Tarefder et al. investigated the effect of dwell time and loading rate on the nanoindentation behavior of asphaltic materials [5]. They found that the unloading portion of the load-displacement curve strongly depends on the dwell time for the long-term aged asphalt binder. After a dwell time of greater than 50s the unloading portion of the load-displacement curve tends to fit Oliver-Pharr analysis with a minimum viscous effect [5, 6].

Instrumented indentation tests involve the utilization of an indenter of known hardness and defined tip shape that penetrates a sample of unknown mechanical property. The forces utilized are in the millinewton range. The indentation area at full load is calculated indirectly by knowing the penetration depth and the known geometry of the indenter [5]. The material tries to regain its shape when the load is removed from the indenter. A measure of elastic modulus is obtained from the shape of the unloading curve. The hardness is obtained from the division of the indentation load by the area of contact [5].

Various models have been introduced to derive the mechanical properties from indentation data. In the work by Doerner and Nix, the authors assumed that the contact area remains constant as the indenter is withdrawn and that the unloading curve is linear and based on such assumptions they were able to introduce a method to calculate hardness from the loading curve and Young's modulus from the unloading curve [6]. On another work by Cheng and Cheng, the development of relationships between elastic modulus, contact area, and initial slope of the unloading curves was carried out based on dimensional analysis of nanoindentation experiments and finite element simulation [7]. On the other hand, for the indentation unloading curves that are not linear at the onset of unloading, Oliver and Pharr refined the Doerner and Nix method to account for that [8].

In the work by Abdelrahman et al., the authors demonstrated the effect of interaction between asphalt, CRM and Virgin Polymer (VP) on the physical properties of the modified asphalt [9, 10]. They proved that depolymerization (of rubber) resulted in the addition of more elasticity to asphalt as evident from the modification of the phase angle. The authors anticipated the development of a network within the binder structure from the value of both G* and δ that are dependent on the material exchange between asphalt, CRM and VP. In another work by Saylak et al., the authors proved the direct relation between the values of the elastic component and the degree of cross-linking of the material that gives the material its elastic characteristics [11].

[1] Department of Civil and Environmental Engineering, North Dakota State University, North Dakota State University, CIE 201, Fargo, ND 58105, USA.
[+] Corresponding Author: E-mail M.abdelrahman@ndsu.edu
Note: Submitted October 29, 2014; Revised February 29, 2015; Accepted March 7, 2015.

The mixing of asphalt with a compatible polymer results in the absorption of the low molecular weight oil fraction of the base asphalt by polymer strands [12]. When these swollen strands connect together at domains or nodes they formalize 3D entangled networks. The mechanical properties of polymer modified asphalts (PMA) and ultimately the asphalt concrete mixes are significantly influenced by these networks [13]. Once destroyed/disturbed by shear flow, such networks can reform with time and impart the ability of self-healing to the PMA [13].

Modification of CRMA occurs by either the swelling of CRM particles through absorbing the light aromatics of asphalt or CRM components release into the liquid phase of asphalt or through the utilization of both mechanisms simultaneously [14, 15]. Severe interaction conditions of combined high interaction temperature and mixing speed result in having the devulcanization and deploymerization processes as major mechanisms leading to the release of the CRM polymeric chains into the asphalt liquid phase [15, 16].

The effect of the control of the interaction parameters between CRM and asphalt on the development of 3D entangled network structure within the liquid phase of CRMA leading to superior rutting and permanent deformation resistance has been previously investigated by the authors [17]. However, up to this point no work has been carried out to investigate the effect of CRMA interaction parameters on its hardness and elastic modulus. Indentation tests would provide data about the hardness and elastic modulus of samples of thickness similar to the actual thickness of asphalt layer laid on aggregate. This would provide a direct approach to anticipate the intrinsic material properties, such as hardness and elastic modulus, of asphaltic materials and mixes during service conditions. The aim of this work is to investigate the effect of interaction parameters of CRMA on their hardness and elastic modulus.

## Materials and Methods

### Materials

In this research work, a single asphalt binder was investigated in combination with one type of crumb rubber modifier (CRM). The asphalt was a PG58-28 (NF) based on superpave grading system. The CRM was a cryogenic processed from a mixed source of scrap tires. The CRM particle size was smaller than mesh #30 and larger than the mesh #40, according to US standard system.

### Methods

#### *Asphalt-CRM Interactions*

The interactions (blend processing) were aimed to investigate the effect of synthesis parameters (mixing speed, temperature and time) on the final product hardness and elastic modulus. Interactions (blend processing) were conducted in 1 gallon cans, and a heating mantle connected to a bench type controller with a long temperature probe (12") was used to heat the material. A high shear mixer was used to mix the asphalt and CRM. The amount of CRM is controlled to be 10%wt of asphalt in all interactions. Interactions were conducted for 8 hours under a combination of three different temperatures (160, 190, and 220℃) and two different mixing speeds (30 and 50 Hz) for each temperature utilized. Samples were taken at 60, 120, 240 and 480 min of interaction time and kept at -12℃ to avoid any unwanted reactions. All interactions in this research were carried out under a blanket of nitrogen gas to prevent any unwanted aging due to oxidation. In addition, the utilization of significant heating temperature is employed as part of the blending processing between asphalt and CRM. A specific coding for the samples was adopted in the current work, starting with the asphalt type, NF, followed by the interaction temperature, interaction speed and lastly the interaction time if required.

#### *Characterization*

**Extraction of Liquid Phase**

In order to make microindentation analysis on the liquid phase (CRMA after removal of CRM particles), the liquid phase of CRMA was extracted by removing the non-dissolved CRM particles from CRMA matrix. In this regard, the required amount of CRMA sample was heated to 165˚C and drained through mesh# 200 (75μm) in the oven at 165˚C for 25 min. The extracted liquid phase was stored at -12˚C immediately to prevent any unwanted reactions.

**Preparation of CRMA Microindentation Samples**

The procedure of asphalt sample preparation for indentation testing was illustrated in the literature [1, 5]. The preparation of the CRMA liquid phase thin film involves the utilization of a glass slide surface that is covered with a high temperature resistant tape. A rectangular window of size 1.5x0.5″ (38.1x12.7 mm) is made inside the high temperature resistant tape. Following that, CRMA is heated to 160℃ and poured into the square window in the high temperature resistant tape. In order to have a smooth CRMA surface, the glass substrate coated with CRMA is placed in the oven at 160℃ for 5 min. After that, the glass substrate is removed out of the oven and cooled down to room temperature. The CRMA film's thickness ranges between 550–600 μm to insure that the measured values for hardness and elastic modulus are not influenced by the glass substrate.

**Microindentation Tests Procedure**

In this research work, a FISCHERSCOPE HM2000S indenter was utilized in the indentation tests. Indentation tests were carried out utilizing a tungsten carbide metal spherical tip of diameter 2mm that conforms with ISO 14577-3. All indentation tests were carried out under load control mode. The indentation load configuration was to start with a constant loading rate followed by a holding period at maximum load and finalizing with an unloading rate similar to the loading one. The maximum load was 5 mN. The loading and unloading times were 20s. The dwell time at maximum load was 60s to minimize the viscous effect on the unloading portion of the material [1, 5, 18]. All tests were carried out at ambient temperature. For each sample a minimum of 5 indentations were carried out to determine the hardness and elastic modulus. A minimum distance of

12 mm between two indentations was utilized to avoid the pile up and sink-in effect for successive indentations and also to conform to the ASTM guidelines of having the required distance of at least 6 indent radii away from the previous indentation point. In this work the utilization of Oliver and Pharr method for the analysis of the indentation test data is carried out [8]. Oliver and Pharr method not only accounts for the curvature in the unloading data but also provides a physically justifiable approach for determining the indentation depth to be used in conjunction with the indenter shape function to establish the contact area at peak load [8]. The analysis starts by defining a reduced modulus Er that accounts for the effects of nonrigid indenter on the load-indentation behavior as follows [19]:

$$\frac{1}{E_r} = \frac{1-v_s^2}{E_s} - \frac{1-v_i^2}{E_i} \quad (1)$$

where $E_s$ = Young's modulus of the sample; $\upsilon_s$= Poisson' s ratio of the sample; $E_i$ = Young's modulus of indenter, $\upsilon_i$ =Poisson's ratio of indenter; and $E_r$ = reduced modulus.

The unloading portion of the indentation curve relates to the reduced modulus as follows [6, 8]:

$$E_r = \frac{\sqrt{\pi}}{2}\frac{S}{\sqrt{A}} \quad (2)$$

where $S$ = d$P$/d$h$ = initial unloading stiffness and A= contact area.

To determine the initial unloading stiffness, Oliver and Pharr utilized curve fitting of the indentation depth versus loading/unloading data using the following power law function [8]:

$$P = \alpha(h - h_f)^m \quad (3)$$

where $h$ = any depth of penetration; $h_f$ = unrecoverable or plastic depth; and α and $m$ = constants.

In this regard, $m$ is a power-law exponent that is related to the geometry of the indenter. The initial unloading slope S is determined by differentiating Eq. (3) and evaluating the derivative at the peak load and displacement [1].

Based on Oliver and Pharr approach, the total displacement h is given as [8]:

$$h = h_c + h_s \quad (4)$$

where $h_c$ is the vertical distance along which contact is made (contact depth) and $h_s$ is the displacement of the surface at the perimeter of the contact [8]. The contact depth $h_c$ can be determined from the experimental data by extrapolating the tangent line to the unloading curve at the maximum loading point down to zero load [1, 8]. $h_s$ can be estimated from the intercept value for depth $h_i$ that relates to the contact depth $h_c$ associated with the maximum loading point as follows [8]:

$$h_c = h_{max} - \varepsilon\frac{P_{max}}{S} \quad (5)$$

where $\varepsilon$ = geometric constant and $P_{max}$ is the maximum indentation load.

The hardness can be obtained as follows [8]:

$$H = \frac{P_{max}}{A} \quad (6)$$

where $A$ = projected area of contact at the peak load.

## Results and Discussion

Fig. 1 illustrates the force vs. indentation depth profiles for the samples interacted at 160℃ with 30 Hz after 1, 2, 4, and 8 hrs of interaction time. As can be seen from Fig. 1, the max load values shows a continuous decrease during the dwell time, similar observations were recorded in the literature for the indentation of asphalt [1]. This was explained in terms of the decrease in contact area due to delayed (viscous) flow of asphalt binders at the indentation location [1]. Another reason is the minute scale load carrying capacity of the asphalt binders and binder softening which results in being virtually impossible to keep the maximum applied load constant [1]. After 1hr of interaction time, the indentation depth was about 50 µm. Increasing the interaction time to 2 and 4 hrs gave almost similar values for the indentation depth of about 45 µm. However, upon increasing the interaction time to 8 hrs, further reduction in the indentation depth was recorded.

Fig. 2 shows the hardness and elastic modulus values for the samples interacted at 160℃ and 30 Hz after 1, 2, 4, and 8 hrs of interaction time. As shown in Fig. 2, a continuous increase in both the hardness and elastic modulus can be seen with the increase of interaction time. The elastic modulus values of samples were 3.21, 3.58, 3.69, and 4.29 MPa, after 1, 2, 4, and 8 hrs, respectively. On the other hand, the hardness values were 0.026, 0.032, 0.038, and 0.065 MPa, after 1, 2, 4, and 8 hrs of interaction time. This indicates that at such combination of interaction temperature (160℃) and interaction speed (30 Hz) the increase in the elastic modulus values occurs gradually with interaction time up to 8 hrs, whereas for the hardness, a major increase occurs from 4 to 8 hrs (almost double the values). This could be as a result of the absorption of the low molecular weight aromatics from the CRMA liquid phase with increase of interaction time by the CRM that leads to stiffer binder [14].

Fig. 3 illustrates the force vs. indentation depth profiles for the samples interacted at 160℃ with 50 Hz after 1, 2, 4, and 8 hrs of interaction time. As can be seen from Fig. 3, the behavior of the indentation depth shows a different trend than that illustrated for the samples interacted at 160℃ and 30 Hz (shown in Figs. 1 and 2). After 1 hr of interaction time, the indentation depth is about 50 µm. However, upon increasing the interaction time to 2, 4, and 8 hrs, we observe almost equal values for the indentation depth ranging around 40 µm. This could be as a result of the increased interaction speed (50 Hz) that resulted in accelerated absorption of the light molecular aromatics that was prevalent after 2 hrs of interaction time, however, it is suggested that because of the low temperature utilized (160℃) an equilibrium status (saturation) is approached that leads to small variation in the indentation depth starting from 2 hrs and up to 8 hrs of interaction time [14].

Fig. 4 shows the hardness and elastic modulus values for the samples interacted at 160℃ and 50 Hz after 1, 2, 4, and 8 hrs of interaction time. As illustrated in Fig. 4, an increase in both the hardness and elastic modulus values is evident after 2hrs of

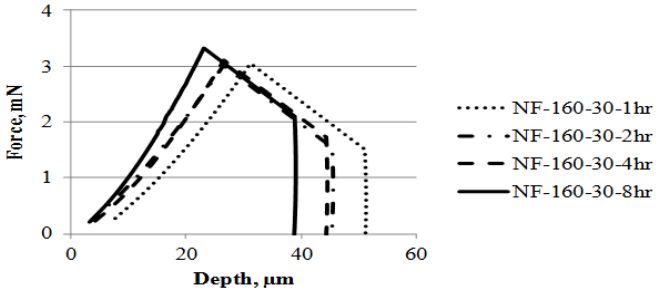


**Fig. 1.** Force vs. Indentation Depth Profile for the Samples Interacted at 160℃ and 30 Hz.

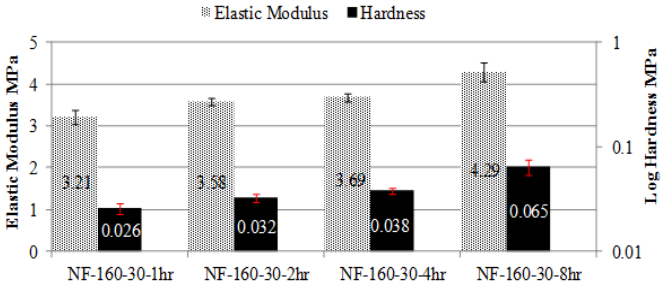


**Fig. 2.** Comparison of Hardness and Elastic Modulus for the Samples Interacted at 160℃ and 30 Hz.

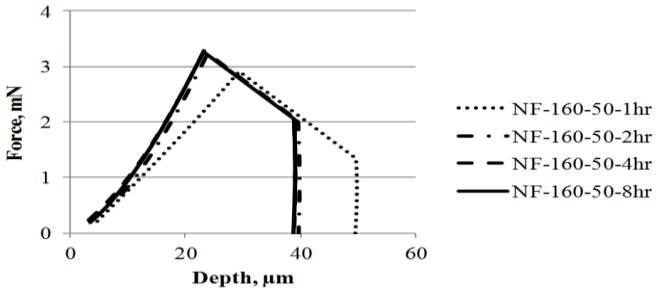


**Fig. 3.** Force vs Indentation Depth Profile for the Samples Interacted at 160℃ and 50 Hz.

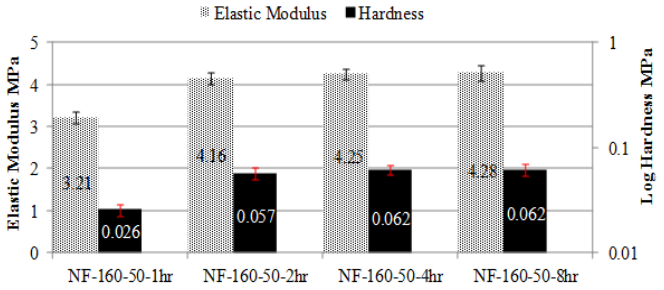


**Fig. 4.** Hardness and Elastic Modulus for the Samples Interacted at 160℃ and 50 Hz.

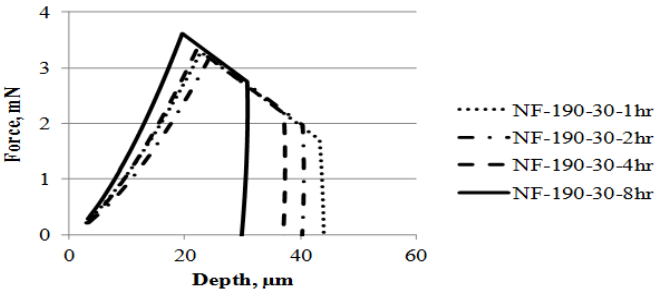


**Fig. 5.** Force vs Indentation Depth Profile for the Samples Interacted at 190℃ and 30 Hz.

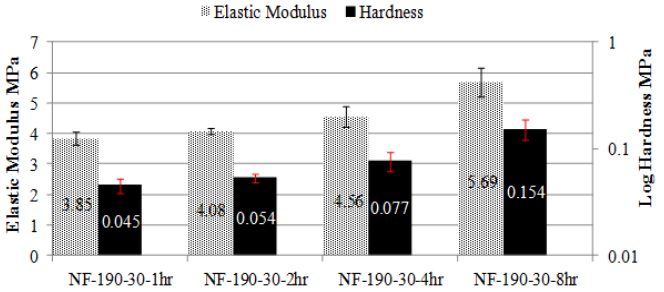


**Fig. 6.** Hardness and Elastic Modulus for the Samples Interacted at 190℃ and 30 Hz.

interaction time. However, minimal increase can be seen for both the hardness and elastic modulus upon the increase from 2 to 4 and 8 hrs. The elastic modulus was 3.21 MPa after 1 hr of interaction time and increased to 4.16, 4.25, and 4.28 MPa, after 2, 4, and 8 hrs of interaction time. The same trend was seen for the hardness values that were 0.026, 0.057, 0.062, and 0.062 MPa, after 1, 2, 4, and 8 hrs of interaction times.

Fig. 5 shows the force vs. indentation depth profiles for the samples interacted at 190℃ with 30Hz after after 1, 2, 4, and 8 hrs of interaction time. As illustrated in Fig. 5, a continuous decrease in the indentation depth can be seen with the increase in interaction time. The interaction depth was about 45 µm after 1hr of interaction time and reached almost 30µm after 8 hrs of interaction time. The indentation depth values for the samples interacted at 190℃ and 30 Hz show more reduction over the samples interacted at 160℃ and 50 Hz after 8hrs of interaction time. This shows that the behavior of the indentation depth shows higher dependency on the interaction temperature that the interaction speed.

Fig. 6 illustrates the hardness and elastic modulus values for the samples interacted at 190℃ and 30Hz after 1, 2, 4, and 8 hrs of interaction time. A gradual increase in the elastic modulus values can be seen with the increase of interaction time. The elastic modulus was 3.8, 4.1, 4.6, and 5.7 MPa after 1, 2, 4, and 8 hrs of interaction time, respectively. On the other hand, the behavior of the hardness followed a different trend. The hardness values were 0.05, 0.05, 0.08, and 0.15 MPa, after 1, 2, 4, and 8 hrs of interaction time. As can be seen from the hardness values, a gradual increase occurred in the first 4hrs of interaction time, whereas the hardness values were almost doubled upon the increase of interaction time from 4 to 8hrs. As explained earlier, this could be as a result of the absorption of the low molecular weight aromatics from the CRMA liquid phase with increase of interaction time by the CRM that leads to stiffer binder. At such interaction conditions of moderate interaction temperature (190℃) and moderate interaction speed (30Hz), the depolymerization and devulcanization effects exerted on CRM are not major and thus the swelling of CRM plays the major role in property modification of CRMA [15, 16, 20].

Fig. 7 illustrates the force vs. indentation depth profiles for the samples interacted at 190℃ with 50Hz after 1, 2, 4, and 8 hours of interaction time. Fig. 7 shows a different trend for the indentation

depth than the previously illustrated samples interacted at either 160℃ (with 30 or 50Hz) or 190℃ with 30 Hz. The indentation depth shows minimal decrease up to 2 hrs of interaction time, however, a major decrease in the indentation depth occurs after 4 and 8 hrs to decrease to almost half the value at interaction time of 8 hrs as compared to 1hr of interaction time. As reported by this research group in earlier research work involving the same samples investigated in this work, this behavior is attributed to the increased devulcanization of CRM with minimal occurrence of depolymerization effects that resulted in the formation of 3D entangled network structures in the liquid phase of CRMA that lead to such major stiffening in the CRMA thus resulting in decreased indentation depth [17, 21].

Fig. 8 illustrates the hardness and elastic modulus values for the samples interacted at 190℃ and 50 Hz after 1, 2, 4, and 8 hrs of interaction time. As illustrated in Fig. 8, the elastic modulus values show a gradual increase from 1(4.3 MPa) to 2 hrs (4.7 MPa) of interaction time. However, starting from 4hrs the elastic modulus values showed major enhancement (8.5 MPa) and was almost double the values of the samples at 2hrs (4.7 MPa). After 8 hrs of interaction time, the elastic modulus was 10.6 MPa. On the other hand, the hardness had a major increase of almost 5 times when the interaction time was increased from 2 hrs (0.09 MPa) to 4 hrs (0.47 MPa). The hardness values continue to increase at 8hrs to be 0.7 MPa. As explained earlier, such distinctive increase in hardness and elastic modulus values after 4 and 8 hrs of interaction time is explained in terms of the development of 3D entangled network structure in the CRMA liquid phase which is associated with such combination of moderate interaction temperature (190℃) and high interaction speed (50 Hz) [17, 21].

Fig. 9 illustrates the force vs. indentation depth profiles for the samples interacted at 220℃ with 30 Hz after 1, 2, 4, and 8 hours of interaction time. As shown in the Figure, a different behavior is observed for the indentation depth with the increase of interaction time. Up to 4hrs of interaction time, the indentation depth shows a continuous decrease. However, after 8 hrs of interaction time, an increase in indentation depth is recorded, indicating that the CRMA is showing less resistance to indentation load. Such behavior can be explained in terms of the increased depolymerization and devulcanization effects occurring for the released CRM components in the CRMA liquid phase that are associated with such interaction temperature (220℃) and even with moderate interaction speed (30 Hz) [15-17].

Fig. 10 illustrates the hardness and elastic modulus values for the samples interacted at 220℃ and 30 Hz after 1, 2, 4, and 8 hrs of interaction time. As illustrated in Fig. 10, the elastic modulus values show a minimal increase from 1 hrs (3.4 MPa) to 2 hrs (3.5 MPa) of interaction time. The enhancement continues up to 4hrs (5.6 MPa). However, at 8hrs of interaction time the elastic modulus values showed reduction (4 MPa). The same behavior was observed for the hardness values. This is explained in terms of the increased deploymerization and devulcanization of CRM released components into the CRMA liquid phase, as explained earlier [15-17].

Fig. 11 illustrates the force vs. indentation depth profiles for the samples interacted at 220℃ with 50 Hz after 1, 2, 4, and 8 hours of interaction time. A more prevalent behavior of increase of indentation depth after 8hrs of interaction time can be observed, indicating the decreased resistance of the CRMA to indentation load.

Fig. 12 illustrates the hardness and elastic modulus values for the samples interacted at 220℃ and 50 Hz after 1, 2, 4, and 8 hrs of interaction time. At 8 hrs of interaction time the elastic modulus values showed a steep reduction (3.8 MPa). The same behavior was observed for the hardness values. This is explained in terms of the

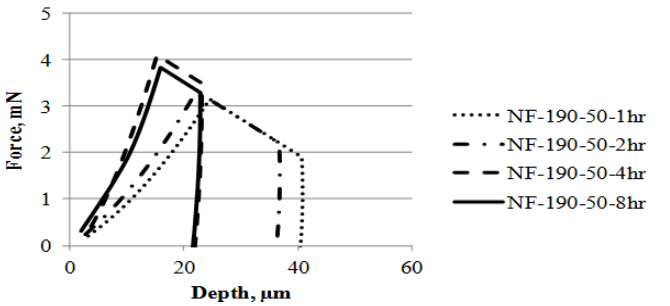


**Fig. 7.** Force vs Indentation Depth Profile for the Samples Interacted at 190℃ and 50 Hz.

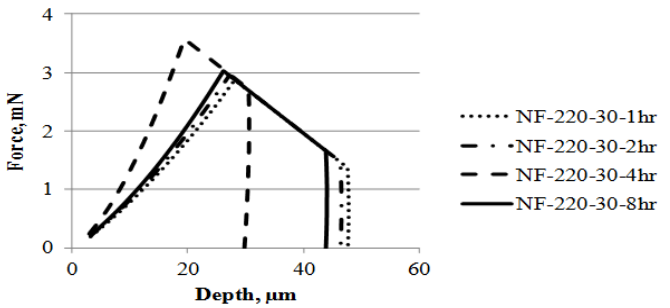


**Fig. 9.** Force vs Indentation Depth Profile for the Samples Interacted at 220℃ and 30 Hz.

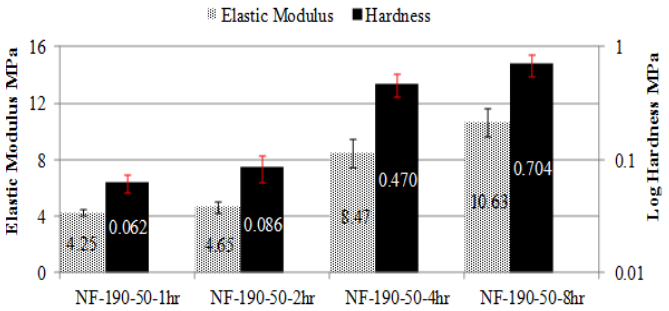


**Fig. 8.** Hardness and Elastic Modulus for the Samples Interacted at 190℃ and 50 Hz.

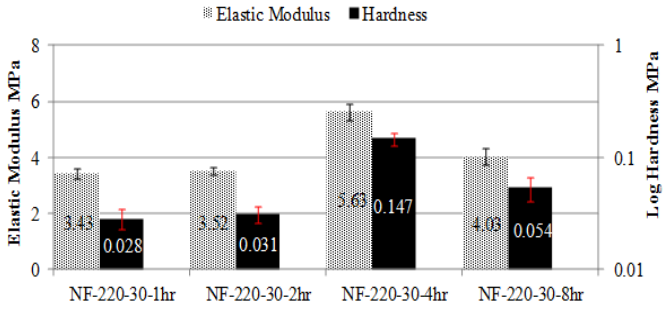


**Fig. 10.** Hardness and Elastic Modulus for the Samples Interacted at 220℃ and 30 Hz.

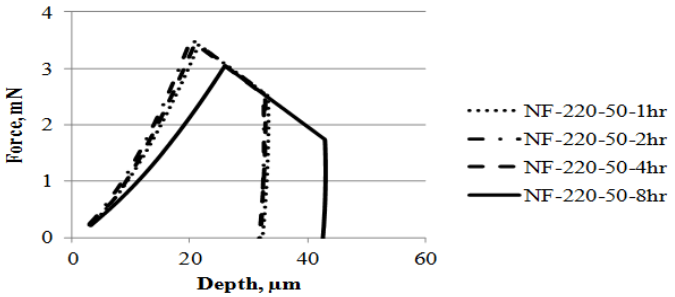


**Fig. 11.** Force vs Indentation Depth Profile for the Samples Interacted at 220℃ and 50 Hz.

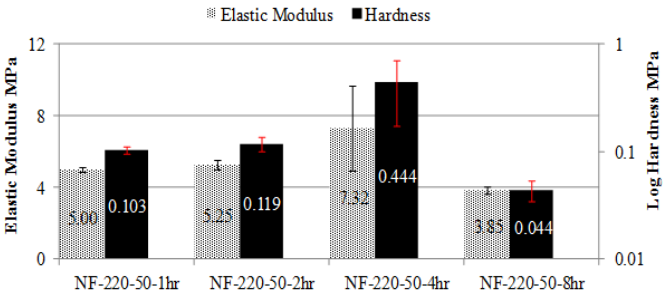


**Fig. 12.** Hardness and Elastic Modulus for the Samples Interacted at 220℃ and 50 Hz.

increased deploymerization and devulcanization of CRM released components into the CRMA liquid phase, as explained earlier [15-17].

## Conclusions

This work investigated the effect of interaction conditions of CRMA on their hardness and elastic modulus. It was found that the utilization of moderate (30 Hz) to high (50 Hz) interaction speeds at low interaction temperature (160℃) resulted in minimal enhancements in both the hardness and elastic modulus as a result of limitation of CRM activities to swelling by absorbance of light aromatics from asphalt. On the other hand, the utilization of moderate (190℃) interaction temperature with high interaction speed (50 Hz) resulted in major property enhancements for both the hardness and elastic modulus as a result of development of 3D entangled network structure in the CRMA liquid phase. At 220℃ interaction temperature, deterioration in both the hardness and elastic modulus was observed after 4 hrs of interaction time regardless of the interaction speed utilized as a result of CRM depolymerization and devulcanization processes that were severe resulting in the annihilation of the CRM modification effects.

## Acknowledgement

This material is based on the work supported by the National Science Foundation under Grant No. 0846861. Any opinions, findings, and conclusions or recommendations expressed in this material are those of the writer(s) and do not necessarily reflect the views of the National Science Foundation.

## References

1. Tarefder, R.A., Zaman, A.M., and Uddin, W. (2010). Determining hardness and elastic modulus of asphalt by nanoindentation. *International Journal of Geomechanics*, 10(3), pp. 106-116.
2. Yousefi, S.S. (2011). Rheological and nanomechanical characterization of aging in polymer modified asphalt, Ph.D. dissertation, University of New Mexico, Albuquerque, New Mexico, USA.
3. Tarefder, R., Faisal, H., and Sobien, H. (2014). Nanomechanical Characterization Effect of Mica and Aging on Asphalt Binder, *Journal of Materials in Civil Engineering*, 26(9), 04014063.
4. Marchildon, R.P. and Hesp, S.A. (2011). Development of microindentation tests for the specification grading of asphalt cements. *International Journal of Pavement Research and Technology*, 4, pp. 222-230.
5. Tarefder, R.A. and Faisal, H. (2012). Effects of dwell time and loading rate on the nanoindentation behavior of asphaltic materials. *Journal of Nanomechanics and Micromechanics*, 3(2), pp. 17-23.
6. Doerner, M.F. and Nix, W.D. (1986). A method for interpreting the data from depth-sensing indentation instruments. *Journal of Materials Research*, 1(04), pp. 601-609.
7. Cheng, Y.-T. and Cheng, C.-M. (1999). Can stress–strain relationships be obtained from indentation curves using conical and pyramidal indenters? *Journal of Materials Research*, 14(09), pp. 3493-3496.
8. Oliver, W.C. and Pharr, G.M. (1992). An improved technique for determining hardness and elastic modulus using load and displacement sensing indentation experiments. *Journal of Materials Research*, 7(06), pp. 1564-1583.
9. Attia, M. and Abdelrahman, M. (2009). Enhancing the performance of crumb rubber-modified binders through varying the interaction conditions. *International Journal of Pavement Engineering*, 10(6), pp. 423-434.
10. Abdelrahman, M. (2006). Controlling performance of crumb rubber-modified binders through addition of polymer modifiers. *Transportation Research Record*, 1962(-1), pp. 64-70.
11. Saylak, D., Noel, J., and Boggess, R. (1978). The Duomorph-An in-situ viscoelastic characterization transducer, In *Verein Deutscher Ingenieure, Internationale Konferenz ueber experimentelle Spannungsanalyse (6th)*, Vol. 1, pp. 279-283.
12. Stroup-Gardiner, M. (1995). Polymer literature review, Interim report, No. *MN/RC-95/27*, Minnesota Department of Transportation, St Paul, MN, USA.
13. Wekumbura, C., Stastna, J., and Zanzotto, L. (2007). Destruction and recovery of internal structure in polymer-modified asphalts. *Journal of Materials in Civil Engineering*, 19, pp. 227.
14. Gawel, I., Stepkowski, R., and Czechowski, F. (2006). Molecular interactions between rubber and asphalt. *Industrial and Engineering Chemistry Research*, 45(9), pp. 3044-3049.

15. Abdelrahman, M.A. and Carpenter, S.H. (1999). Mechanism of interaction of asphalt cement with crumb rubber modifier. *Transportation Research Record*, 1661(1), pp. 106-113.
16. Zanzotto, L. and Kennepohl, G.J. (1996). Development of rubber and asphalt binders by depolymerization and devulcanization of scrap tires in asphalt. *Transportation Research Record*, 1530(1), pp. 51-58.
17. Ragab, M., Abdelrahman, M., and Ghavibazoo, A. (2013). Performance Enhancement of Crumb Rubber-Modified Asphalts Through Control of the Developed Internal Network Structure. *Transportation Research Record*, 2371(1), pp. 96-104.
18. Oyen, M.L. and Ko, C.-C. (2007). Examination of local variations in viscous, elastic, and plastic indentation responses in healing bone. *Journal of Materials Science: Materials in Medicine*, 18(4), pp. 623-628.
19. Stilwell, N. and Tabor, D. (1961). Elastic recovery of conical indentations. *Proceedings of the Physical Society*, 78(2), pp. 169.
20. Ghavibazoo, A. and Abdelrahman, M. (2013). Composition analysis of crumb rubber during interaction with asphalt and effect on properties of binder. *International Journal of Pavement Engineering*, 14(5), pp. 517-530.
21. Wekumbura, C., Stastna, J., and Zanzotto, L. (2007). Destruction and recovery of internal structure in polymer-modified asphalts. *Journal of Materials in Civil Engineering*, 19(3), pp. 227-232.